



# LP Last Stage Steam Turbine Blade Vibrations Due to Mistuning

Leszek Kubitz<sup>1</sup> · Romuald Rzadkowski<sup>1</sup>

Received: 25 September 2016 / Revised: 19 December 2016 / Accepted: 21 December 2016 / Published online: 8 September 2018  
© Krishtel eMaging Solutions Private Limited 2018

## Abstract

**Background** The self-excitation of last stage of slender blades leading to high vibration amplitudes is a problem encountered in the exploitation of LP steam turbines. This has been resolved by changing the geometry of alternate blades (mistuning).

**Method** This paper studies the free and forced blade vibrations of various thus mistuned steam turbine systems. Two methods of mistuning are applied: either by changing the blade geometry or by changing the Young's Modulus.

**Results** In the LP steam turbine last stage, the nodal diameters of blades are destroyed by even the slightest changes to natural blade frequencies and only individual blades vibrate. Blade feathering does make nodal diameters appear, but only in every second blade. The blade geometry mistuning gives more reliable results.

**Conclusions** A comparison of the geometrical and material mistuning reveals completely different results. In the case of long blades, geometrical mistuning is recommended. The maximal blade stress location changes, depending on the form of mistuning.

**Keywords** Dynamics · Steam turbines · Mistuning · Forced vibration

## Introduction

During certain summer low-pressure steam turbine exploitation conditions, excessively high vibrations in the last stage of unshrouded blades were reported.

Rieger [1] presented a review of rotor blade behaviour in a steam turbine, especially in the low-pressure last stage.

Moroz and Romanenko [2] used ANSYS to study the effect of mistuning on LP steam turbine blade high cycle fatigue. Wei-Ze Wang et al. [3] analysed LP steam turbine blade failures, but did take into account multistage coupling.

Rzadkowski and Drewczynski [4] analysed the multistage coupling of eight tuned steam turbine bladed discs on a rotor.

Heinz et al. [5] experimentally examined the circumferential blade amplitude distribution in an LP steam turbine with various operating conditions and mistuning configurations and showed that both have an influence.

Kubin et al. [6, 7] analysed the crack initiation in LP steam turbine blades. The measurements included: torsional excitation of the rotor, blade tip timing, modal analyses, material tests and numerical analysis. In this paper, unstalled flutter was found to be the cause of blade failure.

Rzadkowski and Maurin [8] analysed the multistage coupling of eight mistuned bladed discs on a steam turbine rotor. In this paper, mistuning was found to distort mode shape nodal diameters, mainly in unshrouded bladed discs. It has also shown the importance of multistage coupling between various nodal diameters.

Rzadkowski et al. [9, 10] analysed 3D unsteady forces and flutter in a steam last stage.

Most of the papers on mistuning [11], [12], [13] showed that the level of mistuning is proportionate to the level of bladed disc mode distortion.

Drewczynski et al. [14] numerically studied free vibrations in LP turbine mistuned bladed discs, using two models: geometrical and material mistuning. This showed that the geometrical approach gives completely different mode shapes in the fifth blade vibration series and the even small mistuning completely distorts the nodal diameters.

The paper presented below again compares two methods of blade mistuning, geometrical and material, but the tip timing measured mistuning patterns are different from those in

✉ Romuald Rzadkowski  
z3@imp.gda.pl

Leszek Kubitz  
lokandkod@gmail.com

<sup>1</sup> The Szewalski Institute of Fluid Flow Machinery, Fiszerza 14, 80-952 Gdansk, Poland

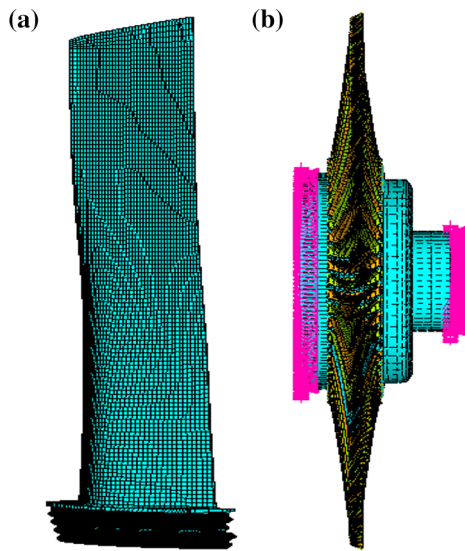


**Fig. 1** **a** FEM mesh of a single cantilever blade; **b** bladed disc model with part of the shaft and boundary conditions

[14]. Also, the method of introducing geometrical mistuning in the FEM is different. Here, the thickness of the upper part of the blade is uniformly changed, in contrast to [14], where only some of the elements were removed.

### Free and Forced Vibration Analysis

The first step was to perform a free vibration analysis of a single blade and tuned bladed disc. The numerical results for the single blade were compared with the modal experimental ones.

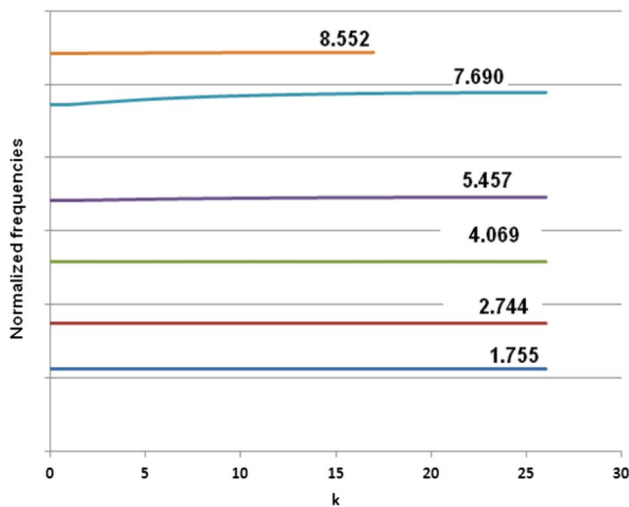


**Fig. 2** Normalized bladed disc frequencies vs. nodal diameter

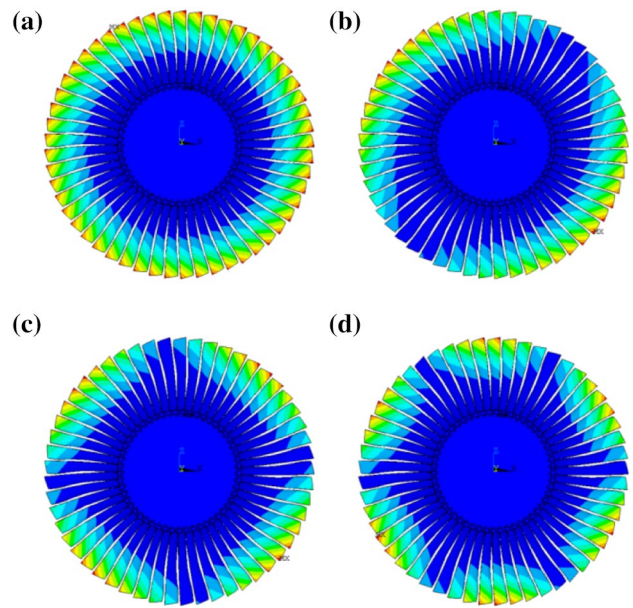


**Fig. 3** The zero **(a)**, first **(b)**, second **(c)** and third **(d)** mode shapes of the tuned bladed disc

The FEM model of the single blade (Fig. 1a) and bladed disc (Fig. 1b) used eight-node quadratic isoparametric brick elements.

The calculated normalized natural frequencies of the stationary cantilever blade were compared with experimental results and were in good agreement for the first five natural frequencies [14].

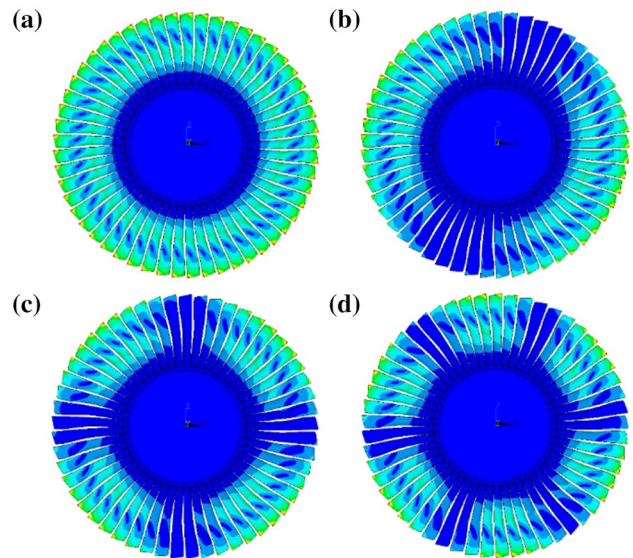


**Fig. 4** The zero **(a)**, first **(b)**, second **(c)** and third **(d)** mode shapes of the fifth series for the bladed disc

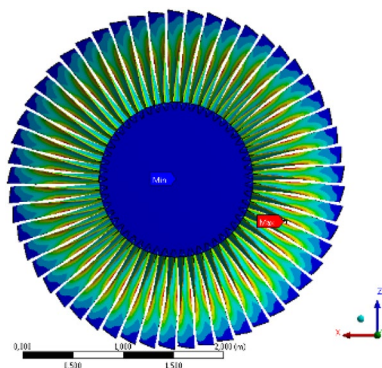


**Fig. 5** Stress amplitude distribution for the tuned bladed disc at 1.764 non-dimensional frequency (zero nodal diameter) in the first vibration series

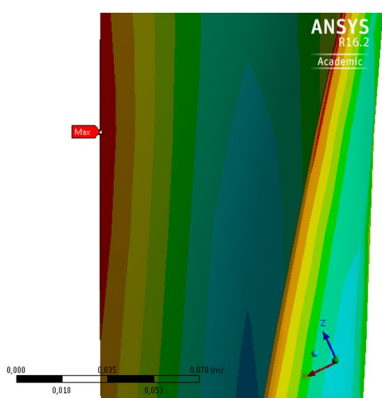


**Fig. 6** Maximum stress amplitude location in a blade of LP turbine tuned bladed disc

The bladed disc FEM model included part of the shaft (Fig. 1b). 15.0 ANSYS was used for the calculations. The inference diagram is presented in Fig. 2.

Figure 3 shows the zero, one, two and three mode shapes of the tuned bladed disc.

Generally, bladed disc modes are grouped into ‘families’ (vibration series). Each family is associated with successive blade cantilever modes (whose natural frequencies converge asymptotically to the natural cantilever blade frequency).

Figure 4 shows the 0, 1, 2 and 3 mode shapes of the fifth series in the tuned bladed disc.

Figures 5 and 6 present the blade stress amplitude distribution (von Mises stress) at 1.764 non-dimensional frequency (zero nodal diameter mode, Fig. 3a). In this case, the maximal stress in the blade occurs in the middle of the leading edge as a result of the blade being twisted by centrifugal forces (Fig. 6).

Two mistuned blade patterns were analysed and in both cases two mistuning approaches were considered. In the first, ‘classical’ approach, blade mistuning was simulated by varying the Young’s modulus (material mistuning). In the second approach, the blade geometry was varied.

### Material Mistuning (0.5 Hz)

Tip-timing measurements were made of the mistuned bladed disc at 3000 rpm (Fig. 7). Blade vibration frequencies mistuned in the region of 0.5 Hz were simulated by changing the blade Young’s modulus. As before, the frequency values were normalized.

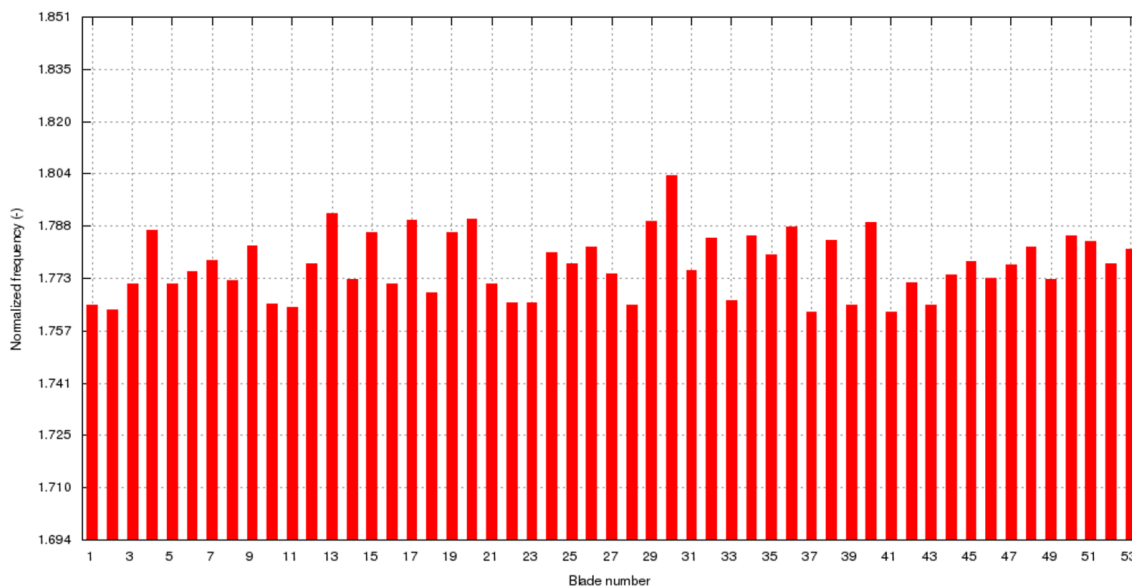


**Fig. 7** Mistuned bladed disc frequencies (in the region of 0.5 Hz) in a real turbine

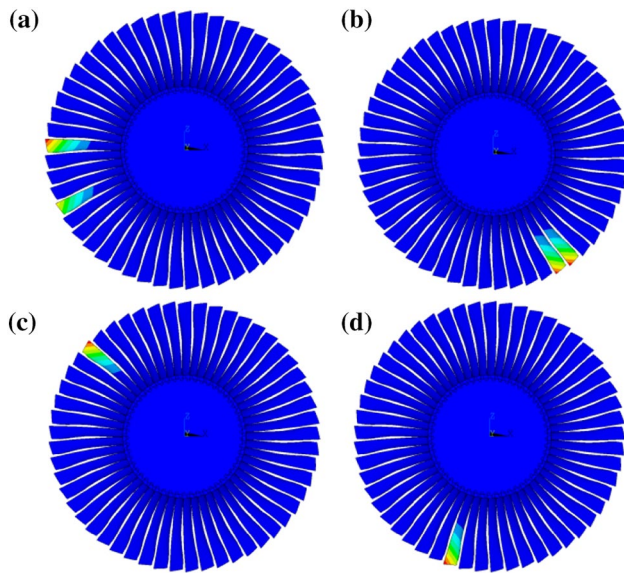


**Fig. 8** Mode shapes of the 0.5 Hz mistuned bladed disc in the vibration first series, 1st (a), 2nd (b), 3rd (c) and 4th (d)

In literature [12, 13], the modes of slightly mistuned bladed discs are generally considered to be similar to those of a tuned bladed disc when the number of nodal diameters is low. With a larger number of nodal diameters, mistuning distorts the nodal lines of the mode shapes. This rule, however, does not hold for long blades.

In contrast to the tuned system modes (Fig. 2), in the mistuned system modes, from the first vibration series, only two blades (Fig. 8a), (Fig. 8b) or one blade vibrated (Fig. 8c,

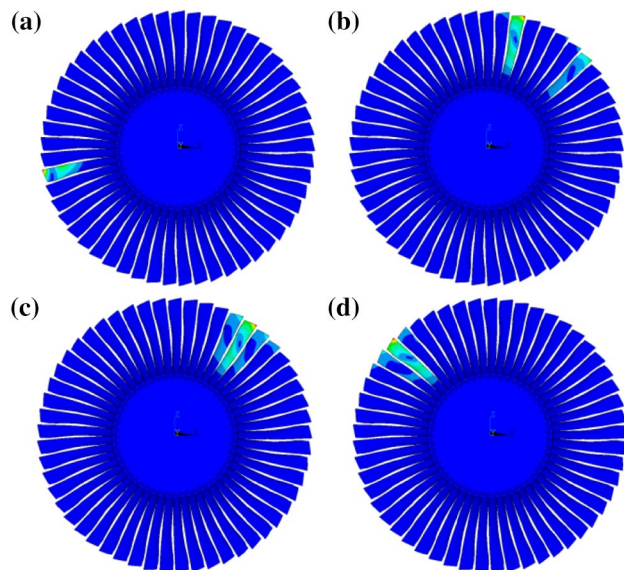


**Fig. 9** Mode shapes of the fifth vibration series: 1st (a), 2nd (b), 3rd (c) and 4th (d)

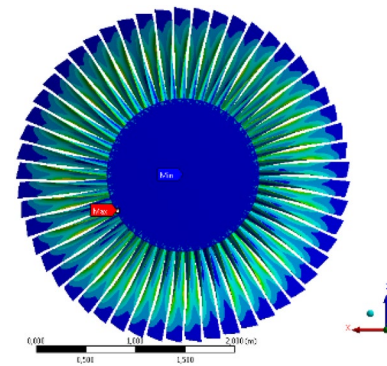


**Fig. 10** Stress amplitude distribution of mistuned bladed disc at 1.767 non-dimensional frequency in the first vibration series

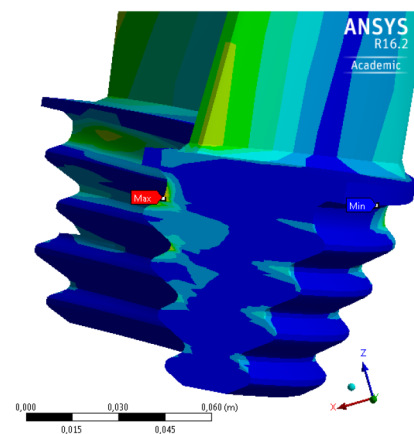


**Fig. 11** Maximum stress amplitude in a single blade at 1.767 non-dimensional frequency in the first vibration series

d), with no visible nodal diameter. A similar behaviour was observed in the second, third, fourth and fifth vibration series (Fig. 9).

In the case of 0.5 Hz mistuning (pattern one), mode shape nodal diameters were not visible even in the fifth vibration series, as was presented in paper [14]. This means that the appearance of nodal diameters in higher modes depends on the mistuning patterns of long blades.

In the forced vibration analysis, the materially mistuned turbine bladed disc was excited by OEO (frequency range from 105 to 115 Hz). The unsteady forces and moment [14] were assumed to be in the blade's centre of gravity. Figure 10 presents the blade stress amplitude distribution (von Mises stress) at 1.767 non-dimensional frequency (Fig. 8a).

The maximal normalized stress in the first vibration series was 1.34, but its localization was in the blade root (see Figs. 10, 11).

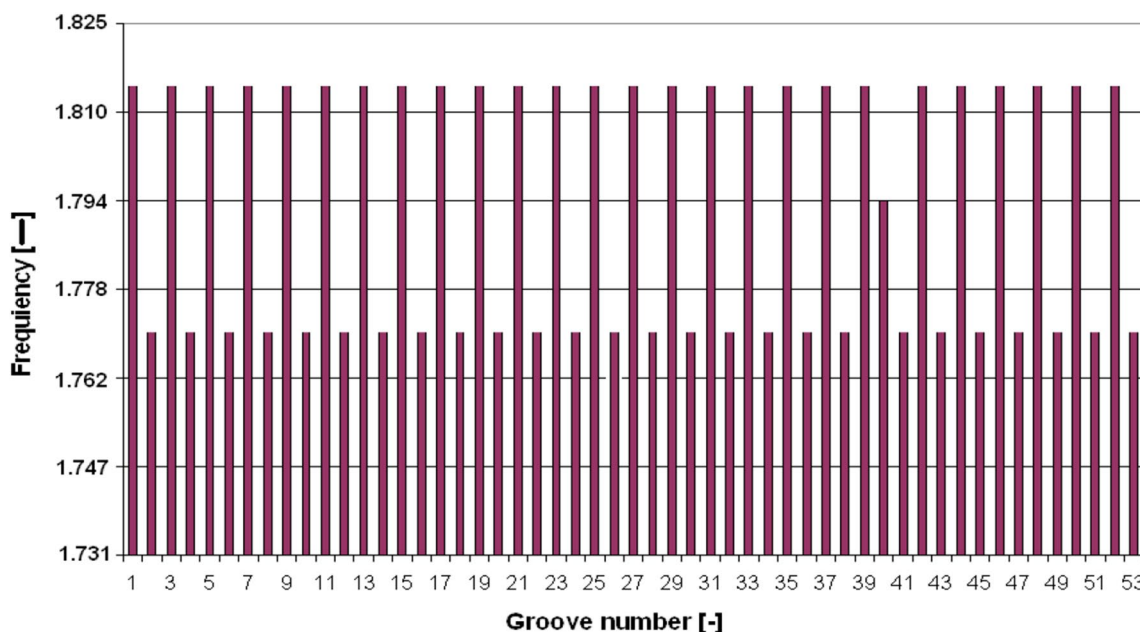


Fig. 12 Theoretical turbine blade frequency distribution in the case of 3 Hz mistuning (feathering)

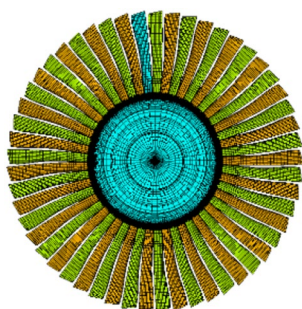


Fig. 13 FEM model of bladed disc after feathering

**Geometrical Mistuning by 3 Hz (Feathering)**

In practice, excessive stress through self-excitation is prevented by slightly reducing the thickness of every other blade tip (feathering), thus lowering their natural frequency by 3 Hz (Fig. 12).

Feathering was introduced to the FEM model by uniformly reducing the thickness of every other blade tip according to the frequency diagram presented in Fig. 12.

Three groups of normalized frequencies were applied: without feathering (1.815, 26 blades), with feathering (1.77, 26 blades) and reference blade 40 (1.794). See Fig. 12.

Figure 13 presents the mistuned bladed disc.

After feathering, the bladed disc mode shapes consisted of a series of 26 modes with 1–13 nodal diameters corresponding to the blade frequencies (1.815,...). Next, there was a series of 26 modes with 1–13 nodal diameters

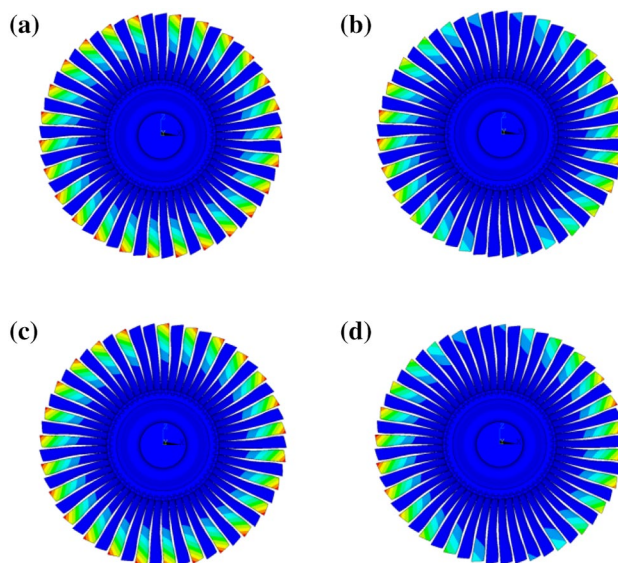
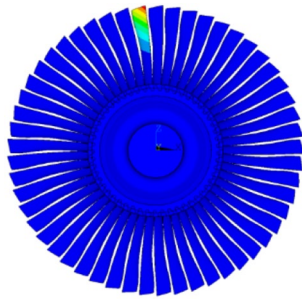


Fig. 14 The 1st (a), 2nd (b), 28th (c) and 29th (d) mode shapes of the 3 Hz (feathering) mistuned bladed disc from the first vibration series, for geometrical mistuning

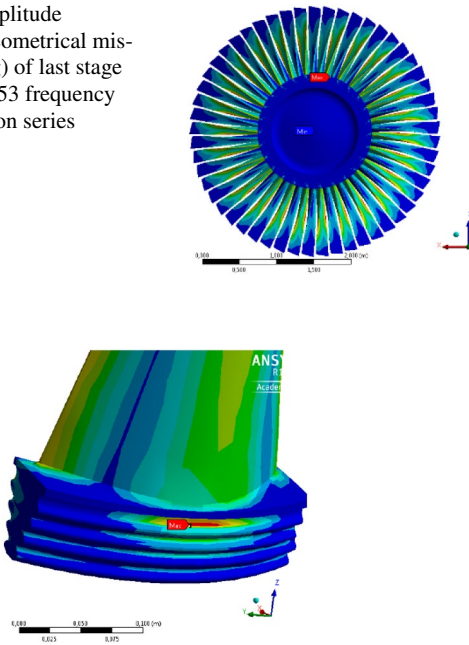
corresponding to blade frequencies (1.766,...) and 1 mode corresponding to blade frequency of 1.794.

Figure 14 presents the 1st, 2nd, 28th and 29th mode shapes of the bladed disc mistuned by feathering from the first vibration series. Nodal diameters appeared in every second blade. In the 27th mode shape, only blade 40 vibrated on account of its different natural frequency (Fig. 15). Mode



**Fig. 15** The 27th mode shape from the first bladed disc vibration series for geometrical mistuning (3 Hz feathering)

**Fig. 16** Stress amplitude distribution for geometrical mistuning (feathering) of last stage bladed disc at 1.753 frequency in the first vibration series



**Fig. 17** Maximum stress amplitude location in a blade for geometrical mistuning (feathering) of the last stage bladed disc

shapes in the 2nd, 3rd and 4th vibration series were similar to those of the 0.5 Hz mistuning (Fig. 8).

In the 5th vibration series, modes shapes with up to the 10 nodal diameters appeared, due to coupling through the bladed disc.

Next, the turbine bladed disc with geometrical feathering was excited by OEO, with frequencies ranging from 105 to 120 Hz. Unsteady blade forces [14] were applied to the blade’s centre of gravity. Figure 16 presents the blade stress amplitude distribution (von Mises stress) at 1.753 non-dimensional frequency (Fig. 17a). The maximal normalized stress at this frequency was 1.04 and located in the blade root. The increase of mistuned blade stress was smaller (4%) than that of the pattern I mistuned bladed disc (34%).

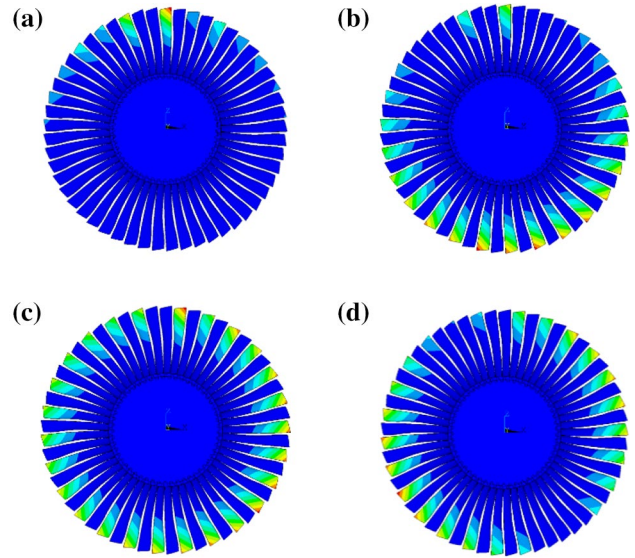


**Fig. 18** Mode shapes of the materially mistuned bladed disc: the 1st (a), 2nd (b), 28th (c) and 29th (d), first vibration series

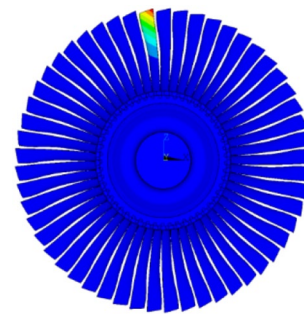


**Fig. 19** The 27th mode shape of the materially mistuned (feathering), first vibration series

### Material Mistuning by 3 Hz (Feathering)

Here, the blade mistuning was simulated by changing the Young’s modulus in accordance with the blade frequencies presented in Fig. 12, without changing the blade geometry.

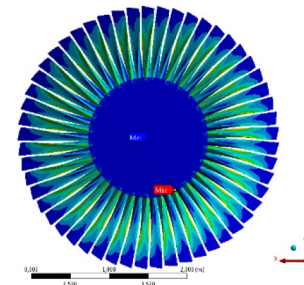


**Fig. 20** Stress amplitude distribution for materially mistuned (feathering) last stage bladed disc at 1.746 frequency in the first vibration series

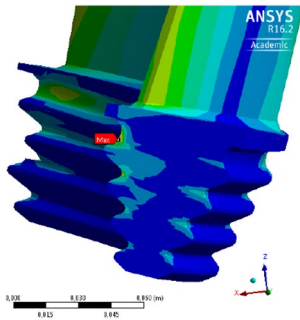


**Fig. 21** Maximum stress amplitude location in a blade for materially mistuned (feathering) last stage bladed disc

Figures 18 and 19 present the 1st, 2nd, 27th, 28th and 29th mode shapes of the mistuned bladed disc in the first vibration series. Unlike geometrical mistuning pattern II (see Fig. 12), here no nodal diameters appeared (see Fig. 18).

The materially mistuned turbine bladed disc (by feathering) was excited by OEO, with frequencies ranging from 105 to 120 Hz. Figure 20 presents the blade stress amplitude distribution (von Mises stress) at 1.746 non-dimensional frequency (see Fig. 18a). The maximal normalized stress in the first vibration series was 0.98, i.e. 2% lower than in the tuned bladed disc. In this case, the material mistuning model did not provide reliable mode shapes and maximal stress values. The blade stress distribution for material and geometrical mistuning was different (see Figs. 17, 21).

## Conclusions

This paper has shown that in the LP steam turbine last stage, the nodal diameters of blades are destroyed by even the slightest changes to natural blade frequencies and only individual blades vibrate. Blade feathering does make nodal diameters appear, but only in every second blade.

The forced vibration analysis has shown that feathering causes lower blade stress in relation to that of a randomly mistuned bladed disc. In comparison to a tuned disc, stress rises by 34% in the case of random mistuning, whereas in the case of the feathered mistuned bladed disc the stress rises by only 4%.

A comparison of the geometrical and material mistuning reveals completely different results. In the case of long blades, geometrical mistuning is recommended.

In this study, we have also found that the location of maximal blade stress in tuned and mistuned bladed disc changes.

**Acknowledgements** Finance for this research came from project Polish Government funds PBS1/B4/5/2012. All numerical calculations were made at the Academic Computer Centre TASK (Gdansk, Poland).

## References

- Rieger NF (2002) Progress with the solution of vibration problems of steam turbine blades, STI Technologies, Inc., 1800 Brighton-Henrietta TL. Rd. Rochester, New York 14623, USA
- Moroz L, Romanenko LG (2003) Vibration analysis of low pressure stages of large steam turbines with ANSYS. SoftInWay Inc., Burlington, p 01803
- Wan W-Z, Xuan F-Z, Zhu K-L, Tu S-T (2007) Failure analysis of the final stage blade in steam turbine, school of mechanical and power engineering, East China University of Science and Technology, Shanghai
- Rzadkowski R, Drewczyński M (2010) Coupling of vibration of several bladed discs on the shaft, part II, forced vibration analysis. *Adv Vib Eng* 9(4):363–374
- Heinz C, Schatz M, Casey MV, Stuter H (2011) Impact of Mistuning on the vibration behaviour of the last stage in a model three stage low pressure steam turbine, ASME 2011 Turbo Expo: Turbine technical conference and exposition, Vol 6, Structures and Dynamics, Parts A and B, Vancouver, British Columbia, Canada, June 6–10, 2011, Paper No. GT2011-45784, pp 1047–1056
- Kubin Z, Cerny V, Panek P, Misek T, Hlous J, Prchlik L (2011) Determination of crack initiation on L-1 LP steam turbine blades: part 1—measurements on rotor train, material specimens and blades, ASME 2011 Turbo Expo: Turbine technical conference and exposition, Vol 6. Structures and Dynamics, Parts A and B, Vancouver, British Columbia, Canada, June 6–10, 2011, Paper No. GT2011-46203, pp 1095–1102
- Kellner J, Kubin Z, Hlous J, Prchlik L (2011) Determination of crack initiation on blade L-1 LP steam turbine blades: part 2—computational analyses, ASME 2011 Turbo Expo: Turbine technical conference and exposition, Vol 6. Structures and Dynamics, Parts A and B, Vancouver, British Columbia, Canada, June 6–10, 2011, Paper No. GT2011-46206, pp 1103–1113
- Rzadkowski R, Maurin A (2014) Multistage coupling of eight mistuned bladed disc on a solid shaft, part 1. Free vibration analysis, ASME Turbo-Expo, Denmark, Copenhagen, Multistage coupling of mistuned aircraft engine bladed disks in a forced vibration analysis, Proceeding of the ASME Turbo Expo 2014, Vol 7. Structure and Dynamics, June 11–15, 2012, GT2014-26108, pp 531–540
- Gnesin V, Kolodyazhnaya L, Rzadkowski R (2004) A numerical model of stator-rotor interaction in a turbine stage with oscillating blades. *J Fluids Struct* 19(8):1141–1153
- Rzadkowski R, Gnesin V (2007) A 3D inviscid self-excited vibration of the last stage turbine blade row. *J Fluids Struct* 23:858–873
- Rzadkowski R, Maurin A (2014) Multistage coupling of mistuned aircraft engine bladed disks in a forced vibration analysis, ASME Turbo Expo 2014: Turbine technical conference and exposition, Vol 7B. Structures and Dynamics Düsseldorf, Germany, June 16–20, 2014, No. GT2014-26108, p V07BT35A016
- Ewins D (1973) Vibration characteristics of bladed disks assemblies. *J Mech Eng Sci* 15(3):165–186
- Rzadkowski R, Surwilo J, Kubitz L, Lampart P, Szymaniak M (2016) Unsteady forces in last stage LP steam turbine rotor blades with exhaust hood, ASME Turbo Expo 2016: Turbomachinery technical conference and exposition, Vol 7B. Structures and Dynamics Seoul, South Korea, June 13–17, 2016, Paper No. GT2016-57610, p V07BT34A020

14. Drewczynski M, Rzadkowski R, Maurin A, Marszalek P (2016) Free vibration of a mistuned steam turbine last stage bladed disc, ASME Turbo Expo 2016: Turbomachinery technical conference and exposition, Vol 7A. Structures and Dynamics, Seoul, South Korea, June 13–17, 2016, Paper No. GT2016-57427, p V07AT32A020